ARTICLE IN PRESS

Engineering Science and Technology, an International Journal xxx (xxxx) xxx

HOSTED BY

ELSEVIER

Contents lists available at ScienceDirect

Engineering Science and Technology, an International Journal

journal homepage: www.elsevier.com/locate/jestch

JESTECH

Full Length Article

Enhanced mechanical properties of AA6061-B_4C composites developed by a novel ultra-sonic assisted stir casting

Suresh Gudipudi [a,1,*], Selvaraj Nagamuthu [a], Kanmani Subbu Subbian [b], Surya Prakasa Rao Chilakalapalli [c]

[a] Department of Mechanical Engineering, National Institute of Technology Warangal, Warangal 506 004, India
[b] Discipline of Mechanical Engineering, Indian Institute of Technology Palakkad, Palakkad 678 557, India
[c] National Institute of Technology Andhra Pradesh, Tadepalligudem 534 102, India

ARTICLE INFO

Article history:
Received 23 October 2019
Revised 16 January 2020
Accepted 27 January 2020
Available online xxxx

Keywords:
Composite
Boron-carbide
Stir-cast
Strength
Sonication

ABSTRACT

The increase of B4C addition into an AA6061-B4C composite system will not be always an ideal choice for improved properties because of the issues related to incorporation, distribution, and interfacial wetting while stir-casting. In such a case, ultrasonication is considered to be an alternative to get the advantage of microstructural changes which in turn improve the properties. In the present study individual B_4C distribution and the refinement of microstructure was achieved at 4wt.%B4C. The improved specific ultimate and compressive strengths at 4wt.%B4C were observed as 36.32% and 43.92% whereas specific Vicker's and Brinell hardness as 53.41% and 50.89% respectively.2009 Elsevier Ltd. All rights reserved.

© 2020 Karabuk University. Publishing services by Elsevier B.V. This is an open access article under the CC BY-NC-ND license (http://creativecommons.org/licenses/by-nc-nd/4.0/).

1. Introduction

Aluminum (Al)/ Al alloy based particulate Metal Matrix Composites (MMCs) are highly demanded in various sectors such as space, defense and automotive due to their high specific strength [1–3]. The Al MMCs are in which Al alloy matrix materials are reinforced with certain amount of hard ceramic reinforcement (RF) particles such as Al_2O_3, SiC, B4C, TiC, TiB_2, etc. Boron carbide (B4C) is the one of such RF materials which exhibits high strength, high hardness, and high melting temperature with low coefficient of thermal expansion [4]. B4C RF particles are also reported for their good chemical stability and bonding characteristics with Al alloys [5]. Therefore, Al alloys are often being reinforced with B_4C to fabricate the MMCs. These MMCs are exhibit low thermal expansion coefficients than pure matrix alloys and hence found suitable for automotive applications [6,7]. Al/Al alloy-B4C MMCs are found in nuclear industry applications as a shielding material because of the high neutron absorption cross-section of B4C [8–14]. The good impact resistance of these MMCs made them suitable in the application of defense sector for making armor components and bullet proof jackets [15–18]. These MMCs are also good choice for marine application by improving corrosion resistance using various post processing (solution heat treatment) techniques [19,20]. The high wear resistance of these MMCs is made them ideal choice for tribological applications [21–24] with the combination of other RF materials known as *hybrid* MMCs [25,26]. These MMCs on which channels made are found in thermal management application for removal of high heat flux [27–29]. There are several methods are being practiced to fabricate the MMCs under broad category of solid state processing (*powder metallurgy* [10,13,14,19,20,30–34]), liquid metallurgical route (molten metal *infiltration* [16], compo/*stir casting* [12,21,22,25,26,28,29,35–45], squeeze casting [7,18,46]), *friction stir process* [23], and laser based *additive manufacturing* technology[24] (selective laser sintering [47–49]).

In solid state *powder metallurgy*, a mix of matrix and RF materials in the powder form is compacted followed by sintering at desired temperature under controlled atmosphere. The MMCs fabricated by this method suffers from a low density and poor RF dispersion. Therefore, this method required of further secondary process like rolling or forging to achieve required density and proper dispersion of RF which in turn offers improved properties. However, the Mg-Zn matrix based bone implant and scaffold porous composites are obtained by this method without requirement of secondary processes. The *Metal injection molding* to get near net complex shape and the *spark plasma sintering* in which the self-heating effect is utilized to get controlled grains growth are other

* Corresponding author.
E-mail address: gudipudi.suresh@gmail.com (S. Gudipudi).
Peer review under responsibility of Karabuk University.
1 ORCID: 0000-0003-4608-664X.

https://doi.org/10.1016/j.jestch.2020.01.010
2215-0986/© 2020 Karabuk University. Publishing services by Elsevier B.V.
This is an open access article under the CC BY-NC-ND license (http://creativecommons.org/licenses/by-nc-nd/4.0/).

Please cite this article as: S. Gudipudi, S. Nagamuthu, K. S. Subbian et al., Enhanced mechanical properties of AA6061-B_4C composites developed by a novel ultra-sonic assisted stir casting, Engineering Science and Technology, an International Journal, https://doi.org/10.1016/j.jestch.2020.01.010

invariants of the *powder metallurgy* [49]. The varying processing conditions which affect the desired property were found in the various published literature. The optimum mechanical alloying time (12 h), compacting pressure (700 MPa) and sintering temperature (635) of a MMC (Al-10 wt.%B4C) for improved relative density (92%), bending strength (160 MPa), and hardness (98HV) were reported by Abinojar et al. [31]. Karako et al. [33] suggested that the required wt.% of B4C for improved fracture toughness (9J), tensile strength (210 MPa), and hardness (70HV) as 10, 5, and 20 respectively. The improvement in the mechanical properties hardness (241HV), bending strength (382 MPa), and compressive strength (438 MPa) of a spark plasma sintering compared to microwave sintering of a Al-15wt.%B4C-1.5wt.%Cobalt MMC was observed by Ghasali et al. [34]. The high-temperature (at 300) mechanical properties of AA6061-5%B4C (hardness:130HV and ultimate strength:120 MPa) and AA7075-5%B4C (hardness: 154HV and ultimate strength: 175 MPa) MMCs were witnessed by Onoro et al. [32]. *Infiltration* is a method in which the liquid matrix material is infiltrated through the preformed RF materials. The disadvantages of this method are residual porosity and unwanted reaction phases at matrix RF particle interface. Arslan et al. [16] reported that the addition of B_4C could decrease the infiltration temperature and the Al_4C_3 reaction phase which could significantly reduce the rate of infiltration while fabricating the Al7075-SiC-B4C MMC. Laser based *additive manufacturing* is an advanced processing technique in which composite powders are fully melted under the irradiation of high-energy laser beam and then solidifies to obtain three dimensional parts. But it suffers from instability of the molten pool, shrinkage, pores and cracks due to a rapid liquid/solid transformation [48]. simulation of the melt pool dynamics and the resultant distribution state of RF (AlN) while selective laser melting of AlN/AlSi10Mg composite has been performed and validated experimentally by Donghua et al. [50]. An optimum linear energy density as 17.5 kJ/m to achieve maximum relative density (96%) of WC/Cu composite fabricated via selective laser melting was reported by Donghua et al. [51].

In *stir casting*, the matrix material is heated above its melting temperature and vortex is created by mechanical stirring through which RF particles are introduced [44]. MMCs fabricated by the *stir casting* have an advantage over powder metallurgy and infiltration methods because of their high density values close to theoretical density and easy control over the composition. Therefore, these MMCs are not required of any further processing (rolling. forging, and extrusion) to achieve high density values. In addition to that, this method overcome the limitation on size of the component to be made and the choice of number of phases compared to powder synthesis route. The *stir casting* is also reported as economical and versatile than powder synthesis route. However, the better distribution of RF particles and higher density (less pores) are achieved by squeezing (secondary process) the stirred composite mix at semi-solid state, named as a *squeeze casting*. The decreased porosity and increased wettability of matrix with RF of Al-5%Cu-7%B_4C composite fabricated using *squeeze casting* were reported by Pozdniakov et al. [7]. *Friction stir processing* is another method to fabricate surface composites which involves a mixing of base matrix and the RF materials in solid state. The improvement in wear resistance (volume loss of 1.36 mm^3) and microhardness (88HV) of AA6061-B4C composite fabricated by the *friction stir process* compared to base material A6061 (volume loss of 5.4 mm^3 and 50HV) was reported by Mehta et al. [23].

In the fabrication of Al alloy matrix based MMCs via *stir casting* method, B4C particles may tend to float on matrix melt due to difference in density values. This tendency would increase at open stirring conditions due to oxide layer formed on top of the melt. Hence, a sufficient stirring speed to be maintained to crate considerable size of the vortex through which B4C particles are incorporated. The addition of suitable flux material of required quantity to the matrix melt would decrease the surface tension matrix alloy. Adoption of several B4C pre-treatment methods would increase the surface energy of B4C. Therefore, both the addition of flux material and the B4C pre-treatment not only improve the ability of B4C incorporation but also ensure the proper bonding between Al alloy matrix and B4C RF. The successful use of flux materials such as K-Al-Ti-F [5253], Cryolite (Na_3AlF_6) [54], Hexachloroethane (C_2Cl_6) [55], and Potassium hexafluorotitanate (K_2TiF_6) [5356] were reported. An optimum B_4C preheating temperature as 250 [35], TiB_2 as a coated material [22], and a special sequential B4C treating method (chemical treatment, ultrasonic cleaning, air drying, oven drying, and milling followed by calcination) [45] were reported in the published literature. Research studies were also focused to identify the possible reaction phases at the particle–matrix interface [57,58,12,43,59]. Various studies to estimate the properties of an Al alloy matrix based B4C MMCs (at varied %B_4C of given particle size) fabricated at varied processing and post-processed [22,60,61] conditions are summarized in the following paragraph.

Kennedy et al. [52] observed that the increased stiffness and modulus values along with the AlB_2 reaction phase for Al-5%B4C MMC. Shorowardi et al. [62] reported that the improved particle dispersion and interfacial bonding could achieve with the preheated B4C for Al-13%B4C MMC. Some reaction phases such as B_2O_3, B_2O_3, Al_2O_3, Al_2O_3, and Al_3BC were also identified by the authors. Canakci et al. [45] also observed that the better particle dispersion and absence of reaction phases in case of the pretreated of B_4C for AA614-x%B4C MMC. Kerti et al. [53] observed that the homogeneous microstructure could not be achieved with the smaller size B_4C (less than 15 μm) for Al-x%B4C MMC. Authors suggested for prolonged holding time and increased mass of flux are necessary to overcome the same issue in case of bigger size (more than 20 μm) and higher (15) weight percentage B_4C. Zhang et al. [57] made some fluidity evolution studies by adding Ti to the AA1100-15% B4C composite slurry. Authors noticed that the decreased fluidity with the long holding time and the increased B_4C clusters due to the growth of reaction phases like Al_3BC and AlB_2. Lashgari et al. [63] reported the increased values of hardness (50%), yield strength (25%), Ultimate Tensile Strength (UTS) (35%) for heat-treated A356-10%B4C composites compared to as cast condition. The increased hardness (105BHN) of heat treated AA6061-10%B4C MMC compared to as cast condition (95BHN) was reported by Rajan et al. [35]. Satyanarayana et al. [55] reported the higher values of both specific hardness (BHN 34.7BHN) and specific UTS (99 MPa) for the heat-treated AA6061-8% B4C composite compared to a similarly heat-treated matrix. Shirvanimoghaddam et al. [54] studied the effect of processing temperature of A356-x%B4C composites on mechanical behavior. The higher UTS (208 MPa) and hardness (93BHN) of the A356-10%B4C composites were observed at 1000 processing temperature compared to 800 . The increased hardness (105HV) up to 20%B_4C of AA6061-x%B4C composite was reported by Thakur et al. [64]. Pozdniakov et al. [12] reported the enhanced distribution of B_4C particles, increased UTS (455 MPa) and hardness (125BHN) of post-processed (heat treated and rolled) 1545 K5-5% B4C composites compared to as-cast conditions. Auradi et al. [65] reported the 38.81% improved tensile (189 MPa) and 32.06% improved compressive (355 MPa) strengths of 6061Al–7% B4C MMC fabricated via two-Stage melt stirring compared to base matrix. Ali Mazahery et al. [22] reported the improved hardness (95HV) and UTS (3 1 5) for TiB_2 coated B4C of post processed (extruded) AA6061-15vol.%B4C compared to uncoated B4C. Ibrahim et al. [43] studied the influence of alloying (Ti, Zr, and Sc) additions on matrix-RF interaction of Al-15 vol% B4C and AA6063-15 vol% B4C. Authors observed that these elements are formed a thin

ARTICLE IN PRESS

protective layers around the B4C which prevent from decomposition. Suresh et al. [25] reported the improved tribological performance of LM25-3%B4C-4%Gr hybrid MMC. Abdizadeh et al [36] reported the optimized parameters for higher UTS 205 MPa (at 10 vol% B4C and 850) and higher hardness 112HV (at 15 vol% B4C and 950) of A356-x%B4C MMC. Subramanya Reddy et al. [37] reported the mechanical properties of AA6061-2%B4C-2%SiC hybrid MMC as 128 MPa (UTS), 214 MPa (flexural strength), 45.8BHN (hardness), and 4.32 J (impact energy). Raj et al. [38] reported the improved mechanical properties at 20vo.% B4C as 124 MPa (yield) and 208 MPa (UTS) of AA6061-x%B4C MMCs. Ulhas et al. [21] reported the improved hardness (74BHN) and UTS (118Mpa) at 3%B4C of AA6061-x%B4C MMCs. Manikandan et al. [26] reported the higher hardness 78BHN and the higher tensile strength 280 MPa at 7.5%B4C and 2.5%CDA (cow dung ash) of AA6061-x%B4C-x%CDA hybrid MMCs. But the high flexural strength (358 MPa) at 2.5%B4C and 7.5%CDA was noticed by authors. Park et al. [41] proposed an automated quantification technique for B4C RF dispersion in Al-x% B4C MMCs. Generally, in the fabrication of MMCs by *stir casting* method, the tendency of particle agglomerations/ clusters increases when the RF size reduces from micro to the nano-level [66]. However, these RF agglomerations were also suspected at micro meter level because of the combined thermal damage (due to surrounding superheated molten metal) and mechanical loading (due to the shearing action of the blade while stirring) effects [64]. The final MMC parts which consist of these RF agglomerations will be surely suspected for their poor mechanical performance. Therefore, this limitation could overcome with a dispersive mixing of the composite mix at liquid state by the application of external fields, such as intensive shearing [67] and ultrasonic cavitation [68–70]. The successful application of ultrasonication as an external field to fabricate nano MMCs was reported [66,68,70–72]. However, this ultrasonication could also improve the properties of the composites (consists of RF particles at micrometer level) [73] and pure matrix metals [74,75].

The fabricating conditions proposed for the improved performance characteristics of MMCs are uncomparable from the reported literature. It is not recommended always to have high B4C content to get improved performance of composite because of the issues associated with the inefficient incorporation, poor dispersion, and complex interfacial reactions. Moreover, the post processing of composite (to avoid these defects) and the pretreatment techniques (to increase the B_4C content to a maximum possible extent) are demand additional cost and time as well. Therefore, adoption of ultrasonication would be the good alternative to get an advantage of microstructural changes which in turn improve the properties even at moderate B4C content. Since the weight percentage (wt.%) of B4C is an important influencing parameter for properties, it is varied between 0 and 8. Therefore, the present study was performed to fabricate the AA6061-B4C MMCs (via ultrasonic assisted *stir casting* at varied wt.%B4C) and to characterize them for estimating the properties (microstructural and mechanical).

2. Materials and methods

2.1. Materials details

Matrix material AA6061 metal pieces were purchased from Bharat Aerospace Metals, Mumbai, India and chemical composition is represented in Table 1. B_4C RF particles having an average size about 30 μm were supplied by Supertek Dies, Delhi, India. As received B_4C particles were analyzed through a scanning electron microscope (SEM) for size and X-ray diffraction (XRD) for purity. Fig. 1(a) shows an SEM image of as-received B_4C particles and their XRD pattern in which major peaks corresponding to B_4C was shown in Fig. 1(b). The properties of AA6061 and B4C are highlighted in Table 2.

2.2. Fabrication of composite

Fig. 2 illustrates the experimental setup used in the present work to fabricate the composites. The AA6061 matrix metal pieces were cut into pieces and cleaned thoroughly. These were heated in graphite crucible up to 750 to achieve a superheated condition in an electrical resistance furnace. The vortex was created by a mechanical stirrer through which the preheated (at 250) B_4C particles and potassium hexafluorotitanate (F_6K_2Ti) flux (about 10% of the weight of B_4C) were introduced to the matrix melt. Experiments were conducted separately for 2, 4, 5, 6 and 8 wt% B_4C. The stirring has to be continued during the B4C incorporation and after complete addition of B4C as well to ensure proper uniform dispersion. Hence the total stir time, (T, min) is to be considered as sum of the B4C incorporation time (T1, min) and time of stirring after completion of B4C addition (T2, min). Authors have performed several pilot experimental trails to observe the distribution of B4C in a molten AA6061 matrix material at varied stirring speeds and times to determine the stirring times. Authors realized that the constant stirring times of T1 and T2 could not yield metal matrix solution with proper distribution of B4C for all wt.% B4C. Hence, the particle feeding and stirring times (T1 and T2) were slightly altered for each weight percentage of B4C by monitoring manually.

The heating and stirring times had an impact on the dispersion of the B4C particles in the metal matrix solution. The sufficient heating time is required to attain the super heat state of AA6061 matrix material to form a complete liquid state of molten pool in order to avoid any un-melted or semisolid matrix material. A very less stirring time could resulting a non-uniform dispersion of B4C whereas the too long stirring time could cause segregation of B4C near the crucible wall due to centrifugal action of vortex. This segregated B4C could agglomerate as a knotty lump sum and left metal matrix solution of no individual B4C particles. The too long stirring time would also lead to erosion of the stirrer blade material which may present in the composite system as another constituent phase in the later stage. The too long stirring time would reduce the size of the B4C. It is because of the combined thermal damage and mechanical loading effects.

The stirrer (stainless steel made) was positioned at one third of height (from the bottom) of composite melt in the crucible. Two stage stirring method is adopted in which the composite melt was stirred for 10 min initially (which include both T1 and T2) for individual distribution of B_4C particulates. Then the composite mix was allowed to cool to reach semi-solid state for 15 min. This semisolid composite was reheated again to 750 followed by stirring for 5 min. The stirring speeds were varied between 300 and 350 rpm based on the B4C incorporation and distribution status which have been continuously monitored. At this stage, the ultrasonic probe (made of titanium alloy of 20 mm dia., generator capacity of 2 kW, Model 1500YV, Johnson Plastosonic, India.) was immersed in the composite mix. This probe generates the high-intensity ultrasonic sound waves of 18 kHz about 15 min in the melt to create a cavitation effect. Therefore, the cavitation bubbles were formed in the liquid matrix melt. These bubbles which are hold at high pressure (more than 100 atmosphere) and high temperature (more than 5000) pulsate intensely within short duration (in microseconds) because of the pressure difference. This would break any B4C clusters present in the composite solution as well as spread homogeneously throughout the liquid metal. Therefore, the improved wettability and random dispersion of

Please cite this article as: S. Gudipudi, S. Nagamuthu, K. S. Subbian et al., Enhanced mechanical properties of AA6061-B_4C composites developed by a novel ultra-sonic assisted stir casting, Engineering Science and Technology, an International Journal, https://doi.org/10.1016/j.jestch.2020.01.010

Table 1
Chemical composition of AA6061 matrix.

Element	Mg	Si	Cu	Mn	Cr	Ti	Zn
Weight (%)	0.88	0.7	0.29	0.33	0.006	0.02	0.003

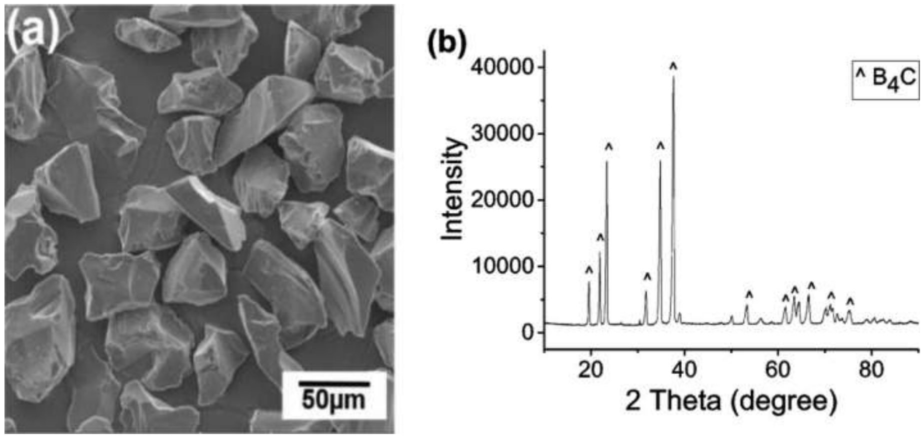

Fig. 1. (a) SEM micrograph of B4C particles (b) XRD analysis of B4C.

Table 2
Properties of AA6061 matrix and B_4C reinforcement materials.

Material	[a]ρ	[b]k	[c]*CTE*	[d]T_m ( )	[e]E (GPa)
AA6061	2.71	180	23	620	70
B_4C	2.51	40	5	2450	450

[a] Density, ρ, (kg/cm^3).
[b] Thermal conductivity, k, (W/ mK).
[c] Coefficient of Thermal Expansion, CTE, (mm × 10^{-6}/m).
[d] Melting Temperature, T_m.
[e] Modulus of Elasticity, E, (GPa).

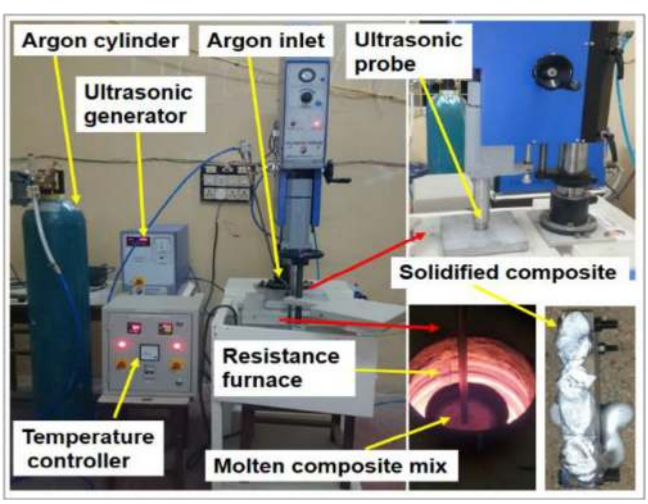

Fig. 2. Photograph for experimental setup of ultrasonic assisted stir-casting process.

B_4C particles in the matrix material were achieved. The MMC mix was poured in the preheated (at 300) split type steel mould having cylindrical and square cross-sectional cavities. The solidified MMC castings were heat-treated (T6 condition). These heat-treated MMCs were machined to standard dimensions for characterization purpose. The photographs of machined composite specimens before and after characterization were shown in Fig. 3.

3. Characterization of composites

The density of composites, 'ρ_{ex}' was measured by using Eq. (1) based on the Archimedes principle. Theoretical density, 'ρ_{th}' was calculated by Eq. (2) by a rule of mix.

$$\rho_{ex} = m/V \tag{1}$$

where ρ_{ex}: experimental or measured density of specimen (g/cm^3); m: mass (g); V: volume of water displaced (cm^3).

$$\rho_{th} = \left[\left(\frac{n_m}{\rho_m}\right) + \left(\frac{n_r}{\rho_r}\right)\right]^{-1} \tag{2}$$

where, ρ_{th}: Theoretical density (g/cm^3), n_m: Weight fraction of matrix material, ρ_m: Density of matrix material (g/cm^3), n_r: Weight fraction of RF material, ρ_r: Density of RF material (g/cm^3).

The relative density 'ρ_{rel}' and amount of porosity level (%) of all specimens Eqs. (3) and (4) respectively.

$$\rho_{rel}(\%) = \left(\frac{\rho_{ex}}{\rho_{th}}\right) \times 100 \tag{3}$$

$$Porosity,\ (\%) = \left[1 - \left(\frac{\rho_{ex}}{\rho_{th}}\right)\right] \times 100 \tag{4}$$

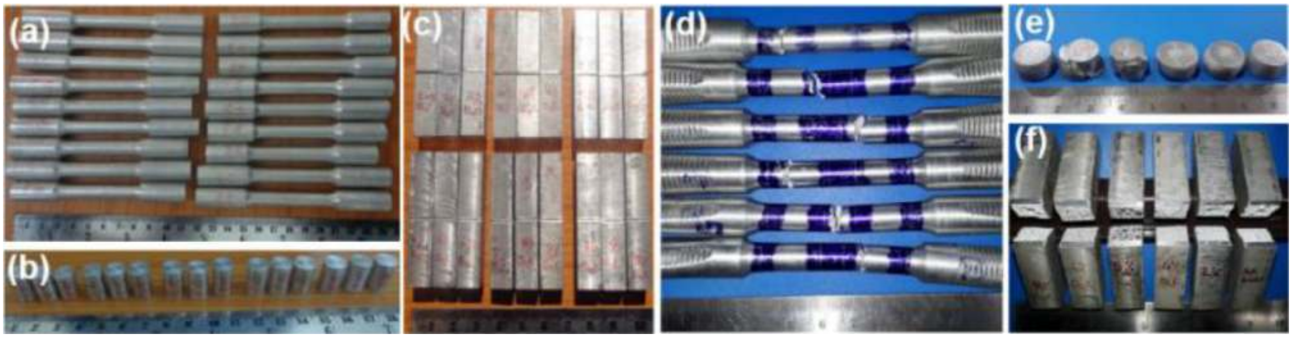

Fig. 3. Photographs of the tensile, compression and impact test specimens: (a) (b) (c) Before testing; (d) (e) (f) After testing.

The uniaxial tensile test (ASTM E8M) was conducted by universal testing machine (250kN capacity, model INSTRON 5985) at a controlled strain rate of 0.01 mm/ mm of gauge length/ sec for 0.2% yield and ultimate tensile strength (UTS). The uniaxial compression test (ASTM E9) was also conducted on the same universal testing machine. The compressive strength was determined for all the specimens by compressing them up to 25% of their initial height at a crosshead speed of 0.5 mm/min. Hardness of the specimens was measured by Shimadzu HMV Vickers micro-hardness tester with diamond indenter having an angle of 136° between opposite faces. The Vickers micro-hardness (HV) is calculated from the Eq. (5) at a load of 500 g with dwell about 15sec.

$$HV = \frac{\{2P\sin(\frac{\alpha}{2})\}}{D^2} \tag{5}$$

where P: load applied (kgf); α: Angle between the two opposite faces of diamond indenter (degrees); *D*: Mean diagonal length of the indentation (mm).

The depth and area of the indentation that covers during the Vickers microhardness (VH) test are limited to few micrometers, hence the surface of the specimen where the indenter was positioned has a great influence on the hardness value particularly in case of multi-phase inhomogeneous composite materials. Therefore, the Brinell hardness test according (ASTM E10) was also conducted on the MMC specimens. The deepest and the widest indentations in this method will be more accurately account for the hardness of the bulk portion. Indentations were made with a steel ball of diameter 10 mm at a load of 500 g about 20 s. Brinell Hardness Number (BHN) was calculated from the following Eq. (6).

$$BHN = \frac{P}{\frac{\pi D}{2}\left[D - \sqrt{D^2 - d^2}\right]} \tag{6}$$

where P: Applied Load (kg); D: Diameter of ball indenter (mm); *d*: Diameter of indentation (mm).

Charpy impact test (ASTM E23) was performed to estimate the impact energy of the specimens. Each Specimen was machined to standard square cross-section 10 mm × 10 mm having a length of 55 mm. V-notch was machined along the middle of the length of the specimen with a notch angle of 45°, 2 mm deep and 0.25 mm root radius. The specimen was kept as a simply supported beam in a horizontal position and loaded behind the notch by the impact of the hammer weighing 18.7 kg with a 140° drop angle at a velocity of 5.3465 m/s. Hence the specimen bends and fractures at high a strain rate. The initial potential energy of Charpy is 300 J. The energy absorbed by the specimen during fracture measured as a difference between the potential energies of the Charpy before and after striking the specimen. The difference was read from the position of the pointer on the scaling dial with the least count of 2 J.

4. Results and discussion

4.1. Process observations

The complete incorporation of B_4C particles into the AA6061 matrix was achieved up to 5 wt% but partially at 6 and 8 wt% B_4C. The reason is, some of the B_4C particles were bonded with matrix and flux materials. The lump of bonded B_4C along with the oxide layer/ slag was ejected from the molten matrix and started to float on the surface of the matrix melt. It was aggregated at the edge of the crucible due to centrifugal action of stirring, hence the molten matrix remained at the bottom of the melt with less number of B4C. The photographs of the ejected B_4C and possible phases identified by XRD analysis were shown in Fig. 4. In the present study the matrix and composite specimens were represented using the codes from Table 3.

4.2. Porosity and microstructure

The variations in the density and the porosity of the matrix and composite were shown in Fig. 5, and it was noticed that the measured density had a lower value than the theoretical one for all the specimens. It is because of the casting defects such as blowholes and pores arise while solidification [45,63]. It is also shown that the level of porosity increased by the addition of B_4C particles up to 4 wt% because of the increased particle content in the composite. The existence of the B_4C particles causes the growth of the surface area and surrounding gas layer (around the particle), which in turn acts as an ideal region for heterogeneous nucleation [55]. The decreased porosity level was observed when B_4C particles were added more than 4 wt% because their agglomeration and ejection from the matrix melt. The difficulty of the B4C incorporation was increased from 6 wt% to 8 wt%, hence the increase of 'ρ_{ex}' and a decrease in porosity values are noticed (Fig. 5).

The optical micrographs for the B_4C distribution pattern and microstructure were shown in Figs. 6 and 7 respectively. The individual B4C dispersion at 2 wt% and 4 wt% were seen from Figs. 6b, and c, 7b and c. Though it was stated that the complete incorporation of B_4C particles was achieved up to 5 wt%, the B4C clusters were formed rather than individual distribution can be observed from Fig. 6d and 7d. A very less number of B4C can be seen for the composites from Fig. 6e and f 7e, and f at 6 wt% and 8 wt% due to particle ejection as explained earlier.

The dendritic microstructure for pure AA6061 matrix was observed from Fig. 7a. The large dendrites were refined when the B4C particle are added which can be seen from Fig. 7b–f. However, the fine refinement of this dendritic microstructure was observed for 4 wt% B4C (Figs. 7c and Fig 8) because it consist relatively more number of individual B4C particles. Fig. 9 shows the EDS analysis of the properly wetted B4C with AA6061 matrix. The formed B4C

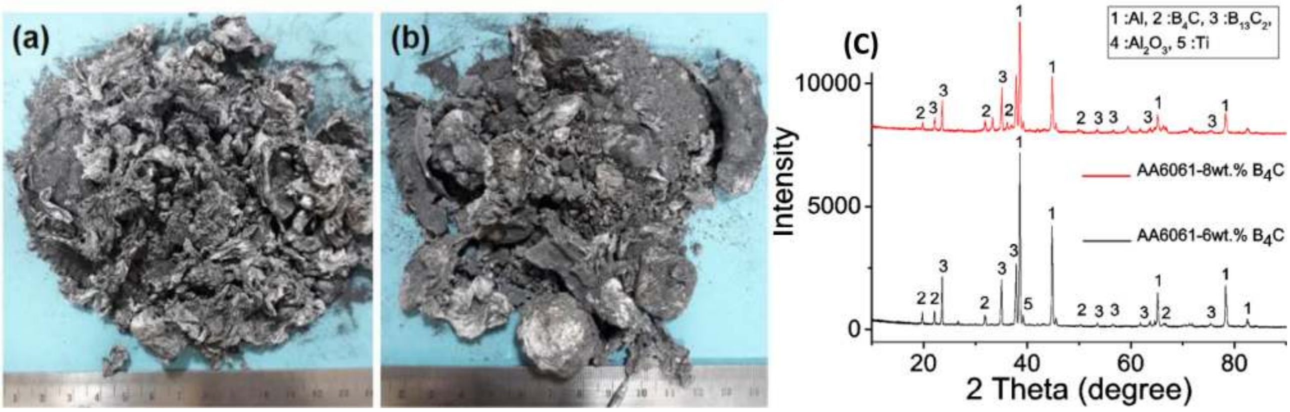

Fig. 4. Photographs of the ejected B4C with slag (a) at 6 wt% B4C (b) 8 wt% B4C (c) XRD analysis of the ejected B4C with slag for possible formed phases.

Table 3
Matrix and composite specimen representation codes.

Speci-men	Pure AA6061	AA6061-2% B_4C	AA6061-4% B_4C	AA6061-5% B_4C	AA6061-6% B_4C	AA6061-8% B_4C
Code	A	B	C	D	E	F

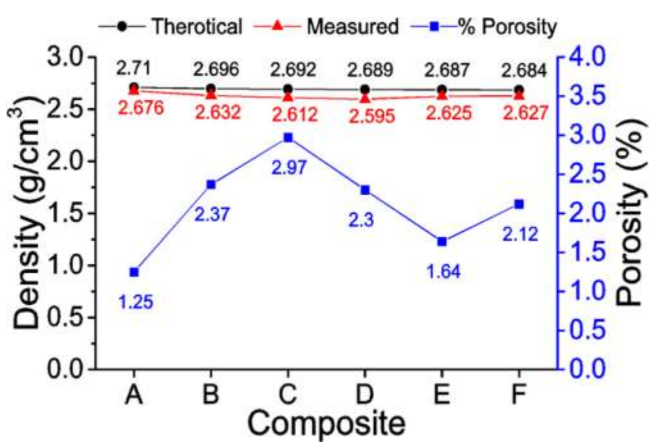

Fig. 5. The density and porosity values of a matrix and AA6061-B4C composites.

clusters were eroded during etching, hence left out pores (Fig. 7d–f) were appeared at 5 wt%, 6 wt%, and 8 wt%.

4.3. Tensile and compressive strength

The tensile and compressive stress–strain curves of the matrix and the composites were shown in Fig. 10a and Fig. 10b respectively. The specific strength (strength/ρ_{ex}) and ductility (% elongation) values were shown in Fig. 11a. The specific compressive strength values were shown in Fig. 11b. The composites of all wt. % B4C are exhibited higher yield strength than pure matrix alloy. Except, the composite at 8 wt% of B4C, the UTS and the compressive strength of all composites are also higher compared to pure matrix AA6061. Various strengthening mechanisms, such as dislocation strengthening, hall–petch strengthening, and strain gradident strengthening are associated with Al alloy-B4C composite system [38].The higher values of the strengths due to the presence of stiffer B4C particles in the matrix material. The B4C particles

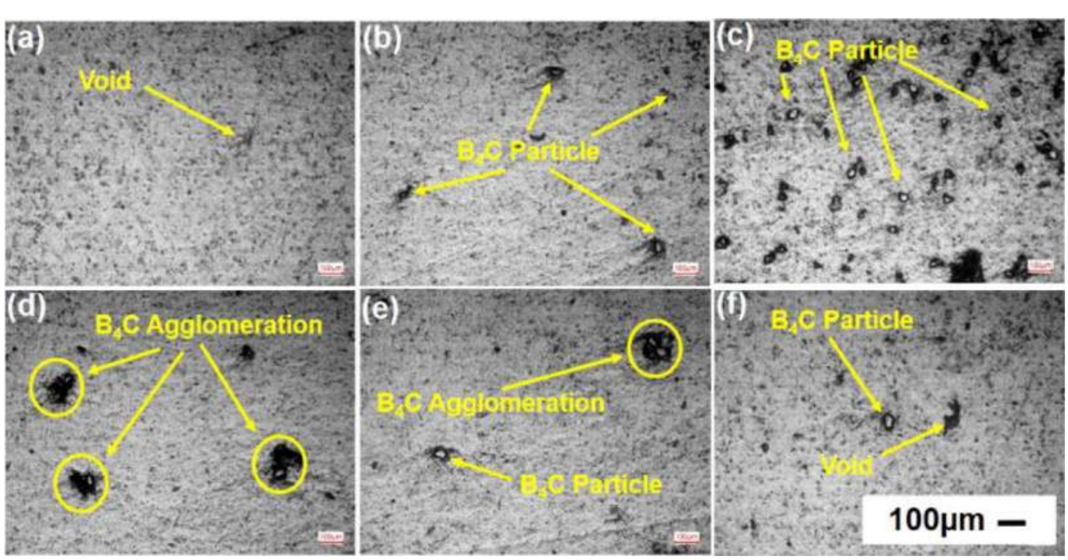

Fig. 6. Optical micrographs for the matrix and distribution of B4C in composite specimens: (a) A (b) B (c) C (d) D (e) E (f) F.

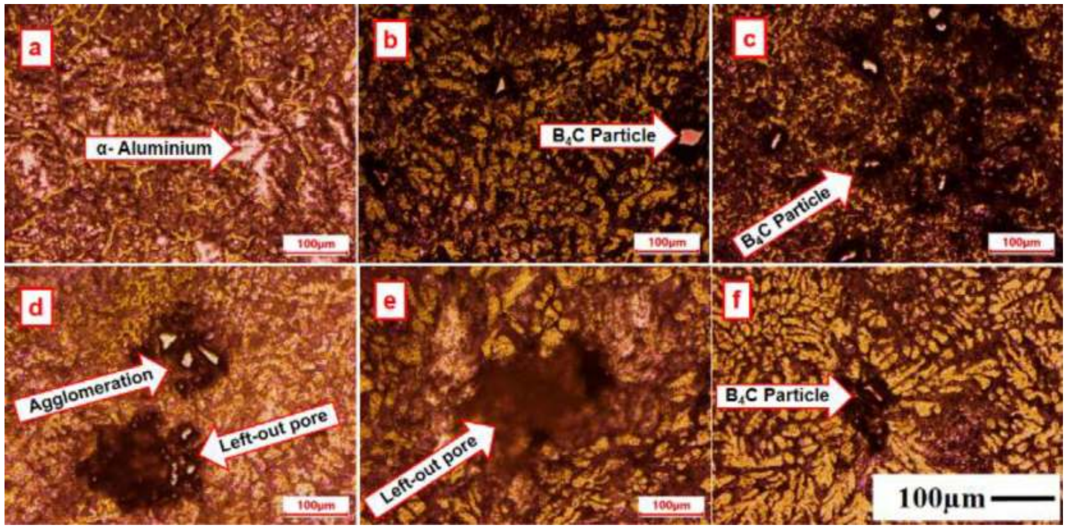

Fig. 7. Optical micrographs for the microstructure and distribution of B4C in composite specimens (a) A (b) B (c) C (d) D (e) E (f) F.

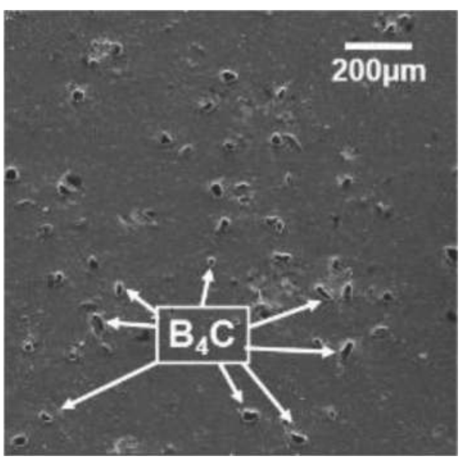

Fig. 8. SEM micrographs for distribution of B4C in AA6061-4% B4C.

cause to increase the resistance against plastic deformation of composites when subjected to loading. Therefore, the effective transfer of load from matrix material to the B4C via the matrix particulate interface is achieved.

The higher wt.% of the B4C particles causes a substantial increase in the dislocation density. The dislocation movements during the test are hindered by the B4C particles and Mg_2Si intermetallic precipitates (formed during heat treatment), hence exhibit more strength. The B4C particles and the AA6061 matrix material are subjected to uneven cooling rate while solidifying from an elevated processing temperature because of the large difference between the thermal expansion coefficient values. Therefore, residual strain were developed. These strain fields would restrict the motion of dislocations when composite subjected to loading. Since, the higher loads are required to move the dislocations around these strain fields, composites exhibit improved strength values. The B4C particles act as artificial nucleation sites, hence the recrystallization of AA6061 matrix occurs by B4C particle stimulated nucleation. The matrix grains are continuous to grow until the B4C particles impede the grain boundary movement. Therefore, the modified microstructure with refined grains of the matrix material is obtained. As a result, the number of grains boundaries (appraisable bonding between B4C particles and matrix material) is increased. At these grain boundaries, the frequent change in the direction of dislocation movement occurs during tensile and compression test. Therefore, the dislocation motion is retarded at grain boundaries, hence strengths are improved. The deformation gradient is created due to the difference in nature of deformation of AA6061 matrix (plastic deformation) and B4C (rigid). The geometrically necessary dislocations (GNDs) which are stored near the B4C surface accommodate these deformation gradients and act as the obstacle to the motion of other dislocations. Therefore these GNDs contribute for the strengthening of composites. However, these composites had a limitation in their strengthening capacity. This limitation arises from the limitation of wt.%B4C which can incorporate into the matrix and the uniformly distributed B4C (properly wetted) particle in the matrix material.

The % increment in specific strength values of composites compared to the AA6061matrix in the present study are represented in Table 4. From the results, it is noticed that the composite at 4%B4C exhibited high strength. The reason is relatively more number of uniformly distributed B4C particles (Fig. 6c) and the refined dendritic microstructure (Fig. 7c). Fig. 13 shows the micrographs of the fractured matrix specimen 'A' (ductile fracture mode) and composite specimen 'C' (brittle fracture mode) during the tensile test.

4.4. Hardness

The variation in specific hardness (hardness/ ρ_{ex}) values of the matrix and composite specimens were graphically represented in Fig. 12a. The more deviation from its mean value of specific HV was observed than specific BHN values for all specimens. Table 5 highlighted the %increment in the specific HV and the BHN values of AA6061-B4C composites compared to the pure matrix AA6061. It was observed that both specific HV and specific BHN values of composites are increased in trend up to 4 wt% B4C (composite 'C') and decreased with a further addition at 5, 6 and 8 wt% of B4C particles. The reason for increasing hardness is the particle crowding (reduced inter-particle spacing) which occur below the indenter during the test. As the individual B4C particle concentration increases, the load transfer capabilit is enhanced. Therefore the composite 'C' at 4 wt% B4C particlesexhibit higher 53.41%, 50.89% in specific HV and BHN respectively than the matrix. Another reason for such high hardness values ecause of precipitation hardening (Mg_2Si precipitates formed during eat treatment) and refinement of microstructure (due to the sonicatin). The decrease in trend of hardness beyond the 4 wt% B4C

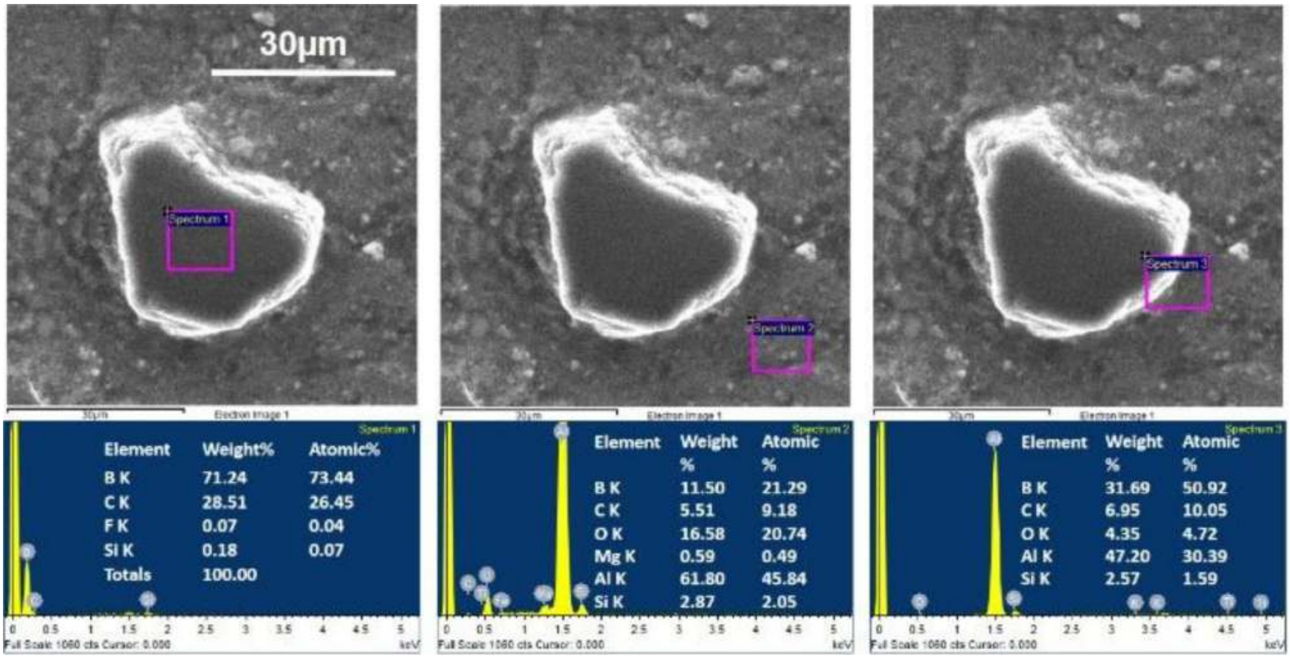

Fig.9. EDS analysis at various regions of the properly wetted B4C with AA6061 matrix.

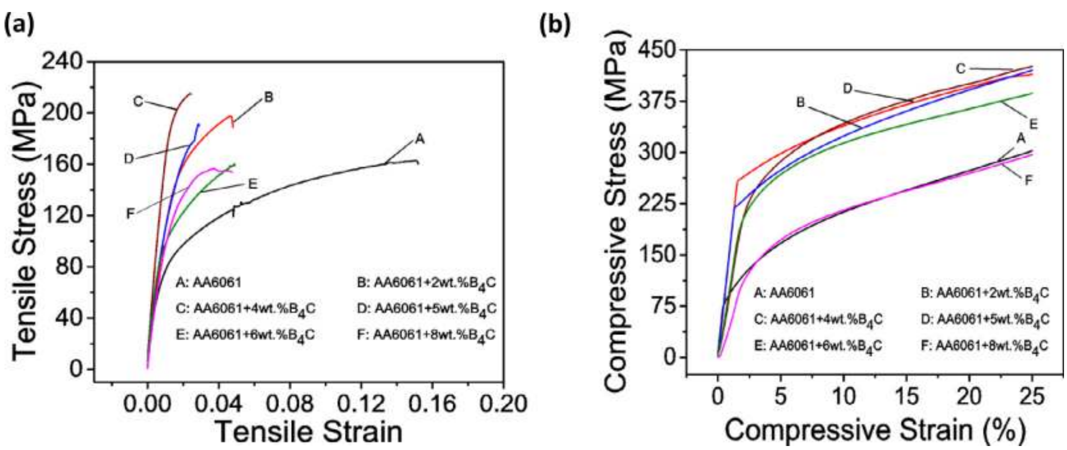

Fig. 10. Stress–strain curves of a matrix and AA6061- B4C composites (a) during tensile test (b) during compression test.

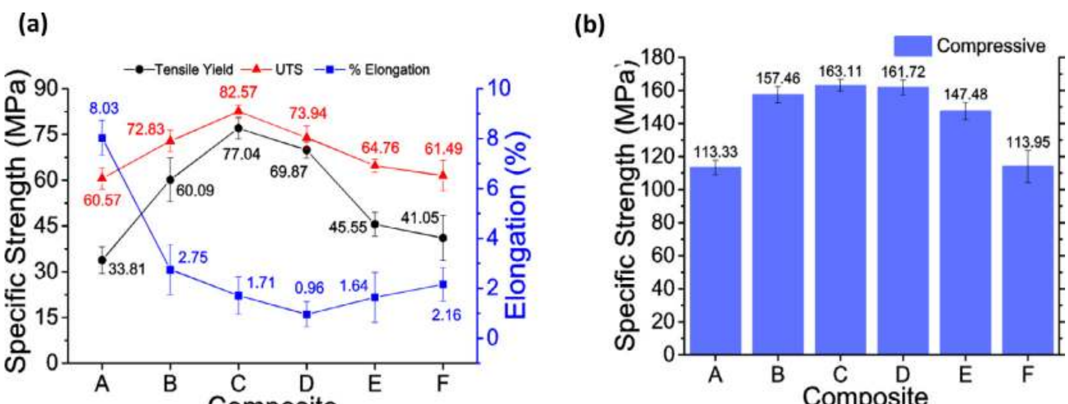

Fig. 11. (a) The variation in % elongation, specific yield, ultimate strength values of a matrix and AA6061- B4C composites (b) The variation in specific compressive strength values of a matrix and AA6061- B4C composites.

Table 4
The percentage (%) increment in specific yield, ultimate, and compressive strength values of AA6061-B4C composites compared to the pure matrix AA6061.

Code	A	B	C	D	E	F
[a]σ_y, (%)	–	77.72	127.87	106.66	34.73	21.42
[b]UTS, (%)	–	20.23	36.32	22.07	6.91	1.49
[c]σ_c, (%)	–	38.93	43.92	42.69	30.13	0.54

[a]Tensile yield strength, (MPa); [b]Ultimate tensile strength, (MPa); [c]Compressive strength (MPa).

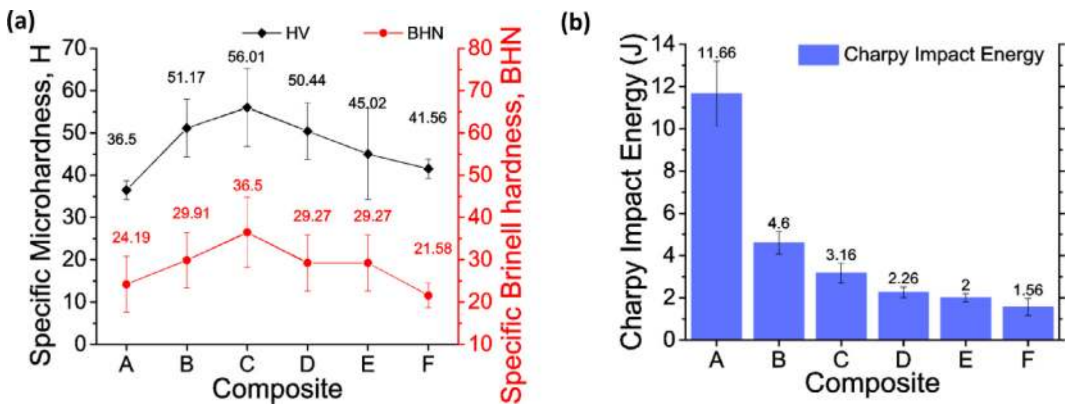

Fig. 12. (a) The variation specific Vickers and Brinell hardness values of a matrix and AA6061- B4C composites (b) The variation in Impact energy values of a matrix and AA6061- B4C composites.

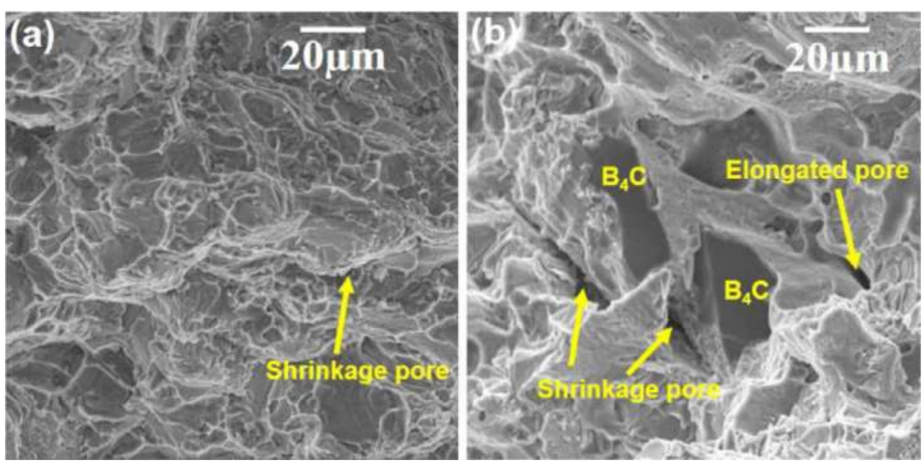

Fig. 13. SEM micrographs of the fractured tensile test specimens of (a) Pure matrix AA6061 (b) AA6061-4 wt% B4C.

Table 5
The percentage (%) increment in specific Vicker's and Brinell hardness values values of AA6061-B4C composites compared to the pure matrix AA6061.

Code	A	B	C	D	E	F
[a]HV, (%)	–	40.17	53.41	38.16	23.33	13.83
[b]BHN, (%)	–	23.67	50.89	21.01	17.92	10.75

[a] The increment in Vicker's hardness number
[b] The increment in Brinnel hardness number.

occur because of the B4C agglomerations. Moreover, these B4C particles tend to segregate towards the eutectic phase, a relatively weaker zone in the composite structure and acts as a crack initiator. However, the higher value of HV and lower value of BHN at 8 wt% B4C (composite 'F') compared to matrix material were observed particles. The reason for this high HV is due to the severe plastic flow which occurs in the localized region. This phenomenon leads to the strain hardening of matrix AA6061 below the indentation. The high hardness is also attributed to the resistance offered by B4C particles which are present in the vicinity of indentation (while the indenter moves downward). But the deepest and the widest indentations in case of Brinell test will be more accurately account for the bulk composite hardness compared to Vickers test. The higher porosity level in the bulk portion of the composite 'F' is a reason for the lower value of BHN compared to the matrix material.

4.5. Impact energy

The variation in impact energy values for matrix and composites were graphically represented in Fig. 12b. The proper individual B4C particle distribution achieved in composites up to 4 wt% and it imparts brittleness to the composite which cannot be reduced much even after heat treatment. Therefore reduction in impact energy values of the composites up to 4 wt% B4C observed from Fig. 12b. The composites developed by further addition of B4C particles beyond 4 wt% which had inherent imperfections in the microstructure due to particle agglomerations and pores, hence less resistance offered to impact loads. Hence the composites D, E, and F showed a decrease in the trend of their impact energy values.

5. Conclusions

The AA6061-B4C MMCs were fabricated via double stir casting method at varied (0, 2, 4, 5, 6, and 8) wt.% B4C. The proper incorporation and distribution of B4C particles into the AA6061 matrix was achieved up to 4 wt% B4C. The ultrasonication was adopted as an external field to the stirred AA6061-B4C MMC mix. The refinement of the dendritic microstructure (due to ultrasonication) in addition to the relatively individual B4C distribution of the composite at 4wt.%B4C exhibited improved mechanical properties. The improvement in specific UTS (36.32%), specific compressive (43.92%), specific VH (53.41%), and specific BHN (50.89%) at such low (4) wt.% of B4C would possible because of the ultrasoication.

Declaration of Competing Interest

The authors declare that they have no known competing financial interests or personal relationships that could have appeared to influence the work reported in this paper.

Acknowledgments

The authors would like to thank the Department of Science and Technology-Science and Engineering Research Board (DST-SERB), New Delhi, India for supporting this work under the Early Career Research scheme (File No. ECR/2017/001320). Authors also would like to thank Shri. D. Rama Lingam, Scientist- E, Advanced Systems Laboratory (ASL) for arranging the tensile and compression test facilities at Materials Development Division (MDD), Defense Research & Development Laboratory (DRDL), Kanchanbagh, Hyderabad, India.

References

[1] D.B. Miracle, Metal matrix composites – From science to technological significance, Compos. Sci. Technol. 65 (2005) 2526–2540, https://doi.org/10.1016/j.compscitech.2005.05.027.

[2] C. Nikhilesh, K.C. Krishan, Metal Matrix Composites, Springer Science Business Media, New York, 2006, p. 266.

[3] P. Mukhopadhyay, Alloy designation, processing, and use of AA6XXX, ISRN Metall. 165082 (2012), https://doi.org/10.5402/2012/165082.

[4] C. Baron, H. Springer, Properties of particle phases for metal-matrix-composite design, Data Br. 12 (2017) 692–708, https://doi.org/10.1016/j.dib.2017.04.038.

[5] J.C. Viala, J. Bouix, G. Gonzalez, C. Esnouf, Chemical reactivity of aluminium with boron carbide, J. Mater. Sci. 32 (1997) 4559–4573, https://doi.org/10.1023/A:1018625402103.

[6] J.N. Fridlyander, Metal Matrix Composites, Chapman & Hall, Russian Academy of Sciences, Moscow, Russia, 1995.

[7] A.V. Pozdniakov, A. Lotfy, A. Qadir, E. Shalaby, M.G. Khomutov, A.Y. Churyumov, V.S. Zolotorevskiy, Development of Al-5Cu/B_4C composites with low coefficient of thermal expansion for automotive application, Mater. Sci. Eng., A 688 (2017) 1–8, https://doi.org/10.1016/j.msea.2017.01.075.

[8] A. Akkaş, A.B. Tugrula, O. Addemira, M. Marşoȷlub, B. Aȷacanb, B. Büyüka, Radiation shielding effect of boron carbide aluminum metal matrix composite, Acta Phys. Pol. A. 127 (2015) 947–949, https://doi.org/10.12693/APhysPolA.127.947.

[9] A. Akkas, A.B. Tugrul, B. Buyuk, A.O. Addemir, M. Marsoglu, B. Agacan, Shielding effect of boron carbide aluminium metal matrix composite against gamma and neutron radiation, Acta Phys. Pol. A. 128 (2015) 176–179, https://doi.org/10.12693/APhysPolA.128.B-176.

[10] J.J. Park, S.M. Hong, M.K. Lee, C.K. Rhee, W.H. Rhee, Enhancement in the microstructure and neutron shielding efficiency of sandwich type of 6061Al-B4C composite material via hot isostatic pressing, Nucl. Eng. Des. 282 (2015) 1–7. doi:10.1016/j.nucengdes.2014.10.020.

[11] J.B. Wierschke, L. Wang, Evaluation of aluminum-boron carbide neutron absorbing materials for interim storage of used nuclear Fuel, A Dissertation of Doctor of Philosophy (2015) 1–159. http://deepblue.lib.umich.edu/bitstream/2027.42/111438/1/jonbrett_1.pdf.2015. [accessed 02 January 2020].

[12] A.V. Pozdniakov, V.S. Zolotorevskiy, R.Y. Barkov, A. Lotfy, A.I. Bazlov, Microstructure and material characterization of 6063/B 4 C and 1545K / B 4 C composites produced by two stir casting techniques for nuclear applications, J. Alloys Compd. 664 (2016) 317–320. doi: 10.1016/j.jallcom.2015.12.228.

[13] H.S. Chen, W.X. Wang, Y.L. Li, P. Zhang, H.H. Nie, Q.C. Wu, The design, microstructure and tensile properties of B4C particulate reinforced 6061Al neutron absorber composites, J. Alloys Compd. 632 (2015) 23–29. doi: 10.1016/j.jallcom.2015.01.048.

[14] H. sheng Chen, W. xian Wang, H. hui Nie, J. Zhou, Y. li Li, P. Zhang, Microstructure and mechanical properties of B4C/6061Al laminar composites fabricated by power metallurgy, Vacuum 143 (2017) 363–370. 10.1016/j.vacuum.2017.06.009.

[15] M. Rosso, Ceramic and metal matrix composites: routes and properties, J. Mater. Process. Technol. 175 (2006) 364–375, https://doi.org/10.1016/j.jmatprotec.2005.04.038.

[16] G. Arslan, A. Kalemtas, Processing of silicon carbide-boron carbide-aluminium composites, J. Eur. Ceram. Soc. 29 (2009) 473–480, https://doi.org/10.1016/j.jeurceramsoc.2008.06.007.

[17] http://eprints.nmlindia.org/2642/1/103-115.PDF [accessed 02 January 2020].

[18] M. Lee, S. Park, I. Jo, S. Lee, Analysis of metal matrix composite (MMC) applied armor system, Procedia Eng. 204 (2017) 100–107, https://doi.org/10.1016/j.proeng.2017.09.761.

[19] N. Kumar, A. Gautam, R. Sevak, S. Manoranjan, K. Manoj, Study of B 4 C / Al – Mg – Si Composites as Highly Hard and Corrosion-Resistant Materials for Industrial Applications, Trans. Indian Inst. Met. 72 (2019) 2495–2501, https://doi.org/10.1007/s12666-019-01717-w.

[20] Q. Bai, L. Zhang, L. Ke, P. Zhu, Y. Ma, S. Xia, B. Zhou, The effects of surface chemical treatment on the corrosion behavior of an Al-B4C metal matrix composite in boric acid solutions at different temperatures, Corros. Sci. 108356 (2019), https://doi.org/10.1016/j.corsci.2019.108356. In press.

[21] U.K. Annigeri, G.B. Veeresh Kumar, Physical, Mechanical, and Tribological Properties of Al6061-B4C Composites, J. Test. Eval. 47 (2019) 20180138. doi: 10.1520/jte20180138..

[22] A. Mazahery, M.O. Shabani, Existence of good bonding between coated B4C reinforcement and al matrix via semisolid techniques: enhancement of wear resistance and mechanical properties, Tribol. Trans. 56 (2013) 342–348, https://doi.org/10.1080/10402004.2012.752552.

[23] K.M. Mehta, V.J. Badheka, Wear behavior of boron-carbide reinforced aluminum surface composites fabricated by Friction Stir Processing, Wear 426–427 (2019) 975–980, https://doi.org/10.1016/j.wear.2019.01.041.

[24] A. Baradeswaran, A.E. Perumal, Influence of B_4C on the tribological and mechanical properties of Al 7075 – B_4C composites, Compos. Part B 54 (2013) 146–152, https://doi.org/10.1016/j.compositesb.2013.05.012.

[25] V. Suresh, N. Hariharan, S. Paramesh, M. Prasath Kumar, P. Arun Prasath, Tribological behaviour of aluminium/boron carbide (B4C)/graphite (Gr) hybrid metal matrix composite under dry sliding motion by using ANOVA, Int. J. Mater. Prod. Technol. 53 (2016) 204–217, https://doi.org/10.1504/IJMPT.2016.079194.

[26] R. Manikandan, T.V. Arjunan, Microstructure and mechanical characteristics of CDA–B4C hybrid metal matrix composites, Met. Mater. Int. (2019), https://doi.org/10.1007/s12540-019-00518-6.

[27] P. Smakulski, S. Pietrowicz, A review of the capabilities of high heat flux removal by porous materials, microchannels and spray cooling techniques, Appl. Therm. Eng. 104 (2016) 636–646, https://doi.org/10.1016/j.applthermaleng.2016.05.096.

[28] S. Gudipudi, N. Selvaraj, D.T.S. Chandra, S.K. Subbu, C.S.P. Rao, A study on geometrical features of electric discharge machined channels on AA6061-4 % B 4 C composites, Measure. Cont. (2020), https://doi.org/10.1177/0020294019888241.

[29] S. Gudipudi, S. Nagamuthu, K.S. Subbian, S.P.R. Chilakalapalli, Fabrication and experimental study to optimize the recast layer and the material removal in electric discharge machining (EDM) of AA6061-B4C composite, Mater. Today Proc. 19 (2019) 448–454, https://doi.org/10.1016/j.matpr.2019.07.634.

[30] R.M. Mohanty, K. Balasubramanian, S.K. Seshadri, Boron carbide-reinforced alumnium 1100 matrix composites: Fabrication and properties, Mater. Sci. Eng. A. 498 (2008) 42–52, https://doi.org/10.1016/j.msea.2007.11.154.

[31] J. Abenojar, F. Velasco, M.A. Martínez, Optimization of processing parameters for the Al + 10% B4C system obtained by mechanical alloying, J. Mater. Process. Technol. 184 (2007) 441–446, https://doi.org/10.1016/j.jmatprotec.2006.11.122.

[32] J. Oñoro, M.D. Salvador, L.E.G. Cambronero, High-temperature mechanical properties of aluminium alloys reinforced with boron carbide particles, Mater. Sci. Eng. A. 499 (2009) 421–426, https://doi.org/10.1016/j.msea.2008.09.013.

[33] Ş. Karabulut, H. Karakoç, R. Çıtak, Influence of B 4 C particle reinforcement on mechanical and machining properties of Al6061/B 4 C composites, Compos. Part B Eng. 101 (2016) 87–98, https://doi.org/10.1016/j.compositesb.2016.07.006.
[34] E. Ghasali, M. Alizadeh, T. Ebadzadeh, Mechanical and microstructure comparison between microwave and spark plasma sintering of Al-B_4C composite, J. Alloys Compd. 655 (2016) 93–98, https://doi.org/10.1016/j.jallcom.2015.09.024.
[35] V.P. Mahesh, P.S. Nair, T.P.D. Rajan, B.C. Pai, R.C. Hubli, Processing of surface-treated boron carbide-reinforced aluminum matrix composites by liquid-metal stir-casting technique, J. Compos. Mater. 45 (2011) 2371–2378, https://doi.org/10.1177/0021998311401086.
[36] H. Abdizadeh, M.A. Baghchesara, Optimized parameters for enhanced properties in Al–B 4 C composite, Arab. J. Sci. Eng. 43 (2018) 4475–4485, https://doi.org/10.1007/s13369-017-2929-9.
[37] P.S. Reddy, R. Kesavan, B. Vijaya Ramnath, Investigation of Mechanical Properties of Aluminium 6061-Silicon Carbide, Boron Carbide Metal Matrix Composite, Silicon 10 (2018) 495–502, https://doi.org/10.1007/s12633-016-9479-8.
[38] R. Raj, D.G. Thakur, Effect of particle size and volume fraction on the strengthening mechanisms of boron carbide reinforced aluminum metal matrix composites, Proc. Inst. Mech. Eng. Part C J. Mech. Eng. Sci. 233 (2019) 1345–1356, https://doi.org/10.1177/0954406218771997.
[39] V.A. Kumar, M.P. Anil, G.L. Rajesh, V. Hiremath, V. Auradi, Tensile and Compression Behaviour of Boron Carbide Reinforced 6061Al MMC's processed through Conventional Melt Stirring, Mater. Today Proc. 5 (2018) 16141–16145, https://doi.org/10.1016/j.matpr.2018.05.100.
[40] X. Li, G.N. Demartino, Dry sliding wear behaviour of Al 7075/ Al_2O_3 / B_4C composites using mathematical modelling and statistical analysis, Mater. Res. Express (2019), https://doi.org/10.1088/2053-1591/ab546a. In press.
[41] B. Park, D. Lee, I. Jo, S.B. Lee, S.K. Lee, S. Cho, Automated quantification of reinforcement dispersion in B4C/Al metal matrix composites, Compos. Part B 181 (2020), https://doi.org/10.1016/j.compositesb.2019.107584.
[42] V. Auradi, G.L. Rajesh, S.A. Kori, Preparation and evaluation of mechanical properties of 6061Al-B 4Cp composites produced via two-stage melt stirring, Mater. Manuf. Process. 29 (2014) 194–200, https://doi.org/10.1080/10426914.2013.872265.
[43] M.F. Ibrahim, H.R. Ammar, A.M. Samuel, M.S. Soliman, F.H. Samuel, Metallurgical parameters controlling matrix/B4C particulate interaction in aluminium-boron carbide metal matrix composites, Int. J. Cast Met. Res. 26 (2013) 364–373, https://doi.org/10.1179/1743133613Y.0000000074.
[44] A. Ramanathan, P.K. Krishnan, R. Muraliraja, A review on the production of metal matrix composites through stir casting – furnace design, properties, challenges, and research opportunities, J. Manuf. Process. 42 (2019) 213–245, https://doi.org/10.1016/j.jmapro.2019.04.017.
[45] A. Canakci, F. Arslan, I. Yasar, Pre-treatment process of B4C particles to improve incorporation into molten AA2014 alloy, J. Mater. Sci. 42 (2007) 9536–9542, https://doi.org/10.1007/s10853-007-1896-z.
[46] A. Mazahery, M.O. Shabani, Mechanical Properties of Squeeze-Cast A356 Composites Reinforced With B 4 C Particulates, J. Mater. Eng. Perform. 21 (2012) 247–252, https://doi.org/10.1007/s11665-011-9867-6.
[47] Y. Yang, X. Guo, C. He, C. Gao, C. Shuai, Regulating degradation behavior by incorporating mesoporous silica for Mg bone implants, ACS Biomater. Sci. Eng. 4 (2018) 1046–1054, https://doi.org/10.1021/acsbiomaterials.8b00020.
[48] C. Shuai, Y. Cheng, Y. Yang, S. Peng, W. Yang, F. Qi, Laser additive manufacturing of Zn-2Al part for bone repair: Formability, microstructure and properties, J. Alloys Compd. 798 (2019) 606–615, https://doi.org/10.1016/j.jallcom.2019.05.278.
[49] Y. Yang, C. He, E. Dianyu, W. Yang, F. Qi, D. Xie, L. Shen, S. Peng, C. Shuai, Mg bone implant: Features, developments and perspectives, Mater. Des. 185 (2020), https://doi.org/10.1016/j.matdes.2019.108259 108259.
[50] D. Dai, D. Gu, Influence of thermodynamics within molten pool on migration and distribution state of reinforcement during selective laser melting of AlN/AlSi10Mg composites, Int. J. Mach. Tools Manuf. 100 (2016) 14–24, https://doi.org/10.1016/j.ijmachtools.2015.10.004.
[51] D. Dai, D. Gu, Thermal behavior and densification mechanism during selective laser melting of copper matrix composites: simulation and experiments, Mater. Des. 55 (2014) 482–491, https://doi.org/10.1016/j.matdes.2013.10.006.
[52] A.R. Kennedy, B. Brampton, The reactive wetting and incorporation of B_4C particles into molten aluminium, Scr. Mater. 44 (2001) 1077–1082. PII: S1359-6462(01)00658-3.
[53] I. Kerti, F. Toptan, Microstructural variations in cast B 4 C-reinforced aluminium matrix composites (AMCs), Mater. Lett. 62 (2008) 1215–1218, https://doi.org/10.1016/j.matlet.2007.08.015.
[54] K. Shirvanimoghaddam, H. Khayyam, H. Abdizadeh, M.K. Akbari, Boron carbide reinforced aluminium matrix composite: Physical, mechanical characterization and mathematical modelling, Mater. Sci. Eng., A 658 (2016) 135–149, https://doi.org/10.1016/j.msea.2016.01.114.
[55] B. Manjunatha, H.B. Niranjan, K.G. Satyanarayana, Effect of mechanical and thermal loading on boron carbide particles reinforced Al-6061 alloy, Mater. Sci. Eng., A 632 (2015) 147–155, https://doi.org/10.1016/j.msea.2015.02.007.
[56] F. Toptan, A. Kilicarslan, A. Karaaslan, M. Cigdem, I. Kerti, Processing and microstructural characterisation of AA 1070 and AA 6063 matrix B_4C_p reinforced composites, Mater. Des. 31 (2010) 87–91, https://doi.org/10.1016/j.matdes.2009.11.064.
[57] Z. Zhang, X.G. Chen, A. Charette, Fluidity and microstructure of an Al-10% B4C composite, J. Mater. Sci. 44 (2009) 492–501, https://doi.org/10.1007/s10853-008-3097-9.
[58] A.R. Kennedy, The microstructure and mechanical properties of Al-Si-B_4C metal matrix composites, J. Mater. Sci. 37 (2002) 317–323. 0022–2461.
[59] Y. Xian, R. Qiu, X. Wang, P. Zhang, Interfacial properties and electron structure of Al/B4C interface: A first-principles study, J. Nucl. Mater. 478 (2016) 227–235, https://doi.org/10.1016/j.jnucmat.2016.06.015.
[60] M. Khademian, A. Alizadeh, A. Abdollahi, Fabrication and characterization of hot rolled and hot extruded boron carbide (B4C) reinforced A356 aluminum alloy matrix composites produced by stir casting method, Trans. Indian Inst. Met. 70 (2017) 1635–1646, https://doi.org/10.1007/s12666-016-0962-0.
[61] H.R. Lashgari, Heat treatment effect on the microstructure, tensile properties and dry sliding wear behavior of A356 – 10 % B_4C cast composites, Mater. Des. 31 (9) (2016) 4414–4422, https://doi.org/10.1016/j.matdes.2010.04.034.
[62] K.M. Shorowordi, T. Laoui, A.S.M.A. Haseeb, J.P. Celis, L. Froyen, Microstructure and interface characteristics of B4C, SiC and Al2O3 reinforced Al matrix composites: A comparative study, J. Mater. Process. Technol. 142 (2003) 738–743, https://doi.org/10.1016/S0924-0136(03)00815-X.
[63] H.R. Lashgari, S. Zangeneh, H. Shahmir, M. Saghafi, M. Emamy, Heat treatment effect on the microstructure, tensile properties and dry sliding wear behavior of A356–10%B4C cast composites, Mater. Des. 31 (2010) 4414–4422, https://doi.org/10.1016/j.matdes.2010.04.034.
[64] R. Raj, D.G. Thakur, ScienceDirect Qualitative and quantitative assessment of microstructure in Al-B 4 C metal matrix composite processed by modified stir casting technique, Arch. Civ. Mech. Eng. 16 (2016) 949–960, https://doi.org/10.1016/j.acme.2016.07.004.
[65] V. Auradi, G.L. Rajesh, S.A. Kori, Preparation and evaluation of mechanical properties of 6061Al- B 4 C p composites produced via two-stage melt stirring, Mater. Manuf. Process. 29 (2) (2014) 194–200, https://doi.org/10.1080/10426914.2013.872265.
[66] L. Poovazhagan, K. Kalaichelvan, T. Sornakumar, Processing and Performance Characteristics of Aluminum-Nano Boron Carbide Metal Matrix Nanocomposites, Mater. Manuf. Process. 31 (2016) 1275–1285, https://doi.org/10.1080/10426914.2015.1026354.
[67] S. Tzamtzis, N.S. Barekar, N.H. Babu, J. Patel, B.K. Dhindaw, Z. Fan, Processing of advanced Al / SiC particulate metal matrix composites under intensive shearing – A novel Rheo-process, Composites, Part A 40 (2009) 144–151, https://doi.org/10.1016/j.compositesa.2008.10.017.
[68] R. Harichandran, N. Selvakumar, Effect of nano / micro B 4 C particles on the mechanical properties of aluminium metal matrix composites fabricated by ultrasonic cavitation-assisted solidification process, Arch. Civ. Mech. Eng. 16 (2016) 147–158, https://doi.org/10.1016/j.acme.2015.07.001.
[69] TMS2013 Annual Meeting Supplemental Proceedings, (2013) 1037–1044.
[70] L. Poovazhagan, K. Kalaichelvan, A. Rajadurai, Preparation of SiC nano-particulates reinforced aluminum matrix nanocomposites by high intensity ultrasonic cavitation process, Trans. Indian Inst. Met. 67 (2014) 229–237, https://doi.org/10.1007/s12666-013-0340-0.
[71] P. Madhukar, N. Selvaraj, R. Gujjala, C.S.P. Rao, Production of high performance AA7150-1% SiC nanocomposite by novel fabrication process of ultrasonication assisted stir casting, Ultrason. Sonochem. 58 (2019), https://doi.org/10.1016/j.ultsonch.2019.104665.
[72] P. Madhukar, N. Selvaraj, C.S.P. Rao, G.B. Veeresh Kumar, Tribological behavior of ultrasonic assisted double stir casted novel nano-composite material (AA7150-hBN) using Taguchi technique 107136, Compos. Part B Eng. 175 (2019), https://doi.org/10.1016/j.compositesb.2019.107136.
[73] J. Ma, J. Kang, T. Huang, Novel application of ultrasonic cavitation for fabrication of TiN / Al composites, J. Alloys Compd. 661 (2016) 176–181, https://doi.org/10.1016/j.jallcom.2015.11.159.
[74] I. Tzanakis, G.S.B. Lebon, D.G. Eskin, K. Pericleous, Investigation of the factors in fl uencing cavitation intensity during the ultrasonic treatment of molten aluminium, Mater. Des. 90 (2016) 979–983, https://doi.org/10.1016/j.matdes.2015.11.010.
[75] W. Khalifa, S. El-Hadad, Ultrasonication effects on the microstructure characteristics of the A380 die cast alloy, Int. J. Met. 13 (2019) 865–879, https://doi.org/10.1007/s40962-018-00296-8.